Chapter V

Solvent induced molecular folding and self-assembled nanostructures of Tyrosine and Tryptophan analogues in aqueous solution

1. Introduction

The environmental concern for the widespread use of a large number of surfactant classes including those of linear alkylbenzene sufonates, alkylphenol ethoxylates and dialkyl quats, leads to legislation in many countries with the aim to gradual phasing out of these materials from commercial and industrial scenario.[1-3] The apprehension is not only due to poor biodegrability under anaerobic conditions concerning the use of anaerobically stabilized sewage sludge as fertilizer in agriculture, but also due to strong inhibitory effects of some of the above surfactant classes on metabolic activity of autotropic ammonia oxidizing bacteria with respect to the nitrogen cycling reaction in soils and water.[4,5] As a result, a trend is quite visible throughout the world to produce more environmentally benign surfactants, although so far only limited success has been achieved to produce the so called green surfactants for industrial purposes at affordable prices. The strategy for preparing environment friendly surfactant molecules could be to start with the biologically active molecules, viz., aminoacids or vegetable oil derivatives.[1,6] The end products of these chemical processes will form the interesting domain of natural surface active biomolecules and create interests not only to chemists and biologists, but also to environmentalists as well.[7-13] These compounds would naturally find a large number of basic and industrial applications too. Since the precursor aminoacid molecules are having biocompatible properties and a large variety of chemical functionalities, the surfactant molecules containing the aminoacids in their molecular architecture would retain the same remarkable properties. Notwithstanding the prevailing situation, the aminoacid based new surfactants would be water soluble, biodegradable, non-toxic, chiral, with little or no adverse impact on soil and aquatic environment.[5-6, 14-16] All these properties ensure their eventual development to cater the need in food, pharmaceutical and cosmetic sectors, which are the major user of various surfactant classes. However, in spite of the promise of optimism that has been raised up in the development of aminoacid based surfactants, volume of industrial production is

still meagre. Further, surprisingly, one of the very important aminoacid class viz., aromatic aminoacids has not been focused for preparing aminoacid based surfactant systems. Therefore, it would indeed be prudent to explore the possibility of surface active properties of long chain derivatives of aromatic aminoacids, especially those of tryptophan and tyrosine, in order to apply these materials as the environment friendly surfactants. This, quite naturally, would not be confined to spherical aggregates and their uses concerning laundry detergent only and rather, the applications of biocompatible and environment-gentle surfactants would be quite diverse. The increasing need for drug delivery systems that improve specificity and activity and at the same time reduce toxicity to ensure maximum treatment safety has led to the development of a great variety of drug vector formation. Since the first reported nonionic surfactants vesicles (ninosomes) at nearly three decade ago, there have been a number of studies on ninosomes as the potential drug carriers, principally focusing on the absence of electrostatic driving force in such systems to create any undesirable secondary interaction interface.[17] The combination of polar aromatic aminoacids and non-polar long chain compounds (esters of tyrosine and tryptophan) might led to the association into vesicles on hydration as a result of existence of a high interfacial tension between water and the hydrocarbon portion of the amphiphile. Therefore, the high promises that are expected to be created for these supramolecular assemblies, if they are formed in aminoacid based systems, would translate into the demand for advanced highly functionalized drug delivery materials having bio-origin.

Another highly challenging fact pertinent to aromatic aminoacid based surfactants, however, prompts also from their biological relevance and strongly functional roles played by aromatic aminoacids in transmembrane proteins at membrane interface. Biological membranes are complex assemblies of lipids and proteins in which phospholipids form the major building blocks. The components of supreme importance in cell membranes are various types of proteins which are associated with lipid bilayer to form functional membranes and perform different important tasks inculcated by the cell. Some crucial of these proteins are either transmembrane proteins, anchored proteins or peripheral proteins. The transmembrane proteins viz., α-helical bundles and β-barrel proteins, localize aromatic aminoacids (especially tyrosine, tryptophan and histidine) at the membrane/water interface where they form functionally significant hydrogen bonds (H-bonds) with interfacial water.[18-23] The discrimination between

nonpolar interior and the polar exterior of the lipid bilayer is made by the transmembrane proteins via the typical hydrophobic and the hydrophilic domains that are present in their molecular architecture. The hydrophobic region which contains a stretch of 20-25 hydrophobic and/or uncharged aminoacids spans the membrane bilayer. The hydrophillic region, on the other hand, are exposed to one or both sides of the membrane, contains hydrophilic aminoacids including aminoacid vesicles. The interplay between hydrophobic and hydrophilic forces in membrane proteins is thus the key to the function and activity of these protein molecules which typically resemble conventional surfactants or amphiphilic molecules in this respect. While amphiphilic behavior of the membrane proteins is indeed significant, it is difficult if not impossible, to study *in situ* because of the inherent complexity of the membrane systems. Long chain alkyl esters of aromatic aminoacids, especially those of tyrosine and tryptophan, could be good models of membrane proteins and a few study on fluorescence behavior of such a model system, viz., tryptophanoctyl ester are reported in literature.[24-29] However, no scientific report of such model systems involving tyrosine or other aromatic amino acids is available. In spite of their importance the surface active property of the model systems have not been reported. Therefore, the initial motivation is to consider the surface activities of long chain esters of tyrosine and tryptophan and to study the behavior of the aromatic π systems at the interface. It is indeed a fact that these materials are not easily available at present, not even from well-known chemical manufacturers. This may be one of the reasons for the lack of interest shown to these model systems. In this chapter, the method of synthesizing octyl esters of tyrosine and tryptophan residues and dodecyl ester of tyrosine and investigation of a detail aspect of the surface activity and related phenomena including their conformations, molecular interactions in aqueous medium, aggregation behavior and the morphology of the self-assembled nano structures of the aggregates are presented.

2. Materials and Methods

2.1. Materials

L-Tyrosinoctyl ester (TYOE), L-Tyrosinedodecyl ester (TYDE) and L-Tryptophanoctyl ester (TROE) were synthesized in our laboratory according to Scheme 1 and Scheme 2 respectively. L-Tyrosine and L-Tryptophan were purchased from HI-Media (India), $SOCl_2$ and n-Dodecanol from Aldrich (USA), n-Octanol from Lancaster

(England). Pyrene was purchased from Fluka (Switzerland) and purified prior to use via column chromatography using Hexane as eluent. Hexane was purchased from SDFCL (India); NaCl, NaOH, Na_2SO_4, for synthesis, were purchased from Merck (India). Purity of all chemicals were greater than 99% and were used as received (except Pyrene). All experiments were done with de-ionised and doubly distilled water with pH 6.5-7 and specific conductance below $2\mu S.cm^{-1}$.

2.2. Methods

2.2.1. Tensiometry. Tensiometric measurements were performed on Krùss K9 Tensiometer (Germany), based on Du-Nóuy ring detachment method, fitted with Omniiset temperature bath with precision ± 0.1^0C. Before each measurement, the platinum ring was thoroughly cleaned with 1:1 acetone-water solution and heated under oxidizing flame until glowing temperature was attained. After every addition, the experimental solution was stirred for 5 minutes for homogeneity and equilibrated for 10 minutes. For each measurement, three to five subsequent readings were taken for concordance. Standard deviation was < 0.1 $mN.m^{-1}$.

2.2.2. pH measurements. The pH's of the solutions were measured using Systronics digital pH meter (Model: 335, India), calibrated with standard buffers of pH 4.0 and 9.2. Solutions were equilibrated for 5 min after addition of alkali till a steady pH meter reading was observed.

2.2.3. **Fluorescence spectroscopy.** Steady state fluorescence emission study was carried out in bench top spectrofluorimeter from Photon Technologies International (Quantamaster-40, USA) with excitation and emission slit widths fixed at 3.0 nm and 2.5 nm respectively. Samples were taken in Hellma quartz cuvette of optical length 1.0 cm.

2.2.4. Nuclear Magnetic Resonance Spectroscopy (NMR). ^{1}H-NMR experiments were performed in Bruker (Germany) ADVANCE spectrometer operating at 300 MHz frequency (for characterisation) and at 400 MHz for 2D ROESY study. Signals are quoted as δ values in ppm using residual protonated solvent signals as internal standard (D_2O: δ 4.79 ppm). Respective solutions were made in D_2O and 0.6 mL of the same was used for each measurement. Data are reported as chemical shift.

2.2.5. High Resolution Transmission Electron Microscopy (HRTEM). HRTEM images were obtained with Jeol JEM 2100 microscope (Japan) operating at accelerating voltage of 200 KV. All images were taken at suitable defocus condition to obtain maximum contrast. A drop of sample solution was added to 200 mesh copper lacey support grid coated with carbon film. Excess sample was manually blotted carefully with Whatman 42 filter paper for 2 s. The grid was dried at 60^0C for 1 hr before experimentation.

2.2.6. Dynamic light scattering (DLS). The dynamic light scattering (DLS) was performed on Zetasizer Nano ZS light scattering apparatus (Malvern Instruments Ltd., UK) with He-Ne laser (632.8 nm, 4 mW) at scattering angle 173^0. The temperature was kept constant at 303 K.

2.3. Synthesis of TYOE and TYDE

To 0.6 mol of n-Alcohol (95 mL n-Octanol; 135 mL n-Dodecanol respectively for TYOE and TYDE) at -5 ^{0} C, 0.055 mol (4 mL) Thionyl chloride was added dropwise and mixture was stirred for 10 min (Scheme 1). To this, 0.05 mol (9 g) of L-Tyrosine was added and the resulting mixture was stirred and refluxed at 95 ^{0} C for 21 hrs under nitrogen atmosphere. The mixture was then allowed to stand at room temperature. The white solid that appeared was washed with diethylether several times (to remove excess n-alkanol) and filtered via vacuum suction. It was then dissolved in water and pH was adjusted to 7 (± 0.2) by dropwise addition of ~ 0.1N NaOH solution. The white cloudy solution was taken in a separating funnel to which ethyl acetate was added and mixture was shaken well and kept to stand overnight. Clear, transparent layer of water and ethyl acetate was obtained.

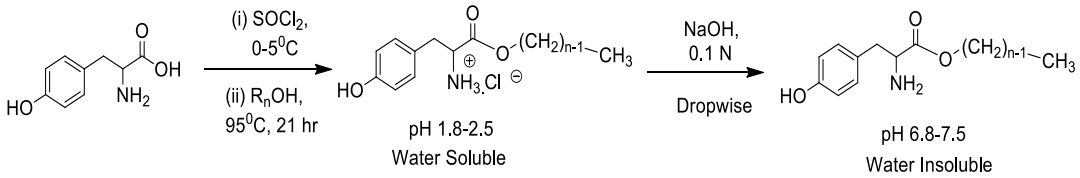

Scheme 1: Synthetic route of L-Tyrosine alkyl ester, n=8 (TYOE), 12 (TYDE)

The organic part of the mixture was collected over Na_2SO_4 and solvent was evaporated in a water bath and product was dried in vacuum pump for 6 hrs.[30] Yellow semisolid product for TYOE (Yield ~72%, 6.5 g) and white crystalline product for TYDE (Yield

~75%, 6.7 g) were respectively obtained and these were characterized using ^{1}H and ^{13}C NMR Spectroscopy.

L-Tyrosine Octyl ester:

^{1}H-NMR (300 MHz, $CDCl_3$): δ (ppm) 7.3 (1H, -OH), 7.01 (d, 2H, 8.4 Hz), 6.69 (dd, 2H, 2.1 Hz), 4.17-4.10 (m, 2H), 3.74-3.66 (m, 1H), 3.2 (broad, $-NH_2$), 3.05 (dd, 1H, 5.1 Hz), 2.94-2.79 (m, 1H), 2.06 (t, 2H), 1.64 (t, 2H), 1.31-1.25 (m, 10H), 0.898 (t, 3H, 6.6 Hz)

^{13}C-NMR (300 MHz, $CDCl_3$): δ (ppm) 174.9, 130.35 (for two C, twice intensity), 127.9, 115.7, 77.45, 77.02, 76.60, 65.43, 55.54, 39.71, 29.18, 28.55, 25.88, 22.62, 14.17, 14.07.

L-Tyrosine Dodecyl ester:

^{1}H-NMR (300 MHz, $CDCl_3$): δ (ppm) 7.2 (s, -OH), 6.99 (d, 2H, 8.4 Hz), 6.66 (d, 2H, 8.4 Hz), 4.12 (t, 2H, 6.6 Hz), 3.71 (q, 1H, 5.1 Hz), 3.03 (broad, $-NH_2$), 3.05 (dd, 1H, 4.8, 5.1 Hz), 2.8 (q, 1H, 7.1 Hz), 1.63 (t, 2H, 6.6 Hz), 1.28 (d, 18H, 5.1 Hz), 0.88 (t, 3H, 6.3 Hz).

^{13}C-NMR (300 MHz, $CDCl_3$): δ (ppm) 174.9, 155.4, 130.34, 127.79, 115.77, 77.46, 77.03, 76.61 65.46, 55.53, 39.71, 31.91, 29.63, 29.58, 29.51, 29.34, 29.24, 28.57, 25.89, 22.68, 14.11.

2.4. Synthesis of TROE

To 63 mL (0.4 mol) n-Octanol maintained at -5^{0}C, 2.2 mL $SOCl_2$ (0.03 mol) was added dropwise and stirred for 30 minutes. Thereafter, 6 g L-Tryptophan (0.03 mol) was added and the mixture was stirred and refluxed at 130^{0}C under nitrogen atmosphere for 21 hrs. The white solid obtained was washed with diethyl ether several times and dried.[31] It was then treated with ethyl acetate and strong NaOH solution was added dropwise to adjust pH to 7.0 (± 0.2)

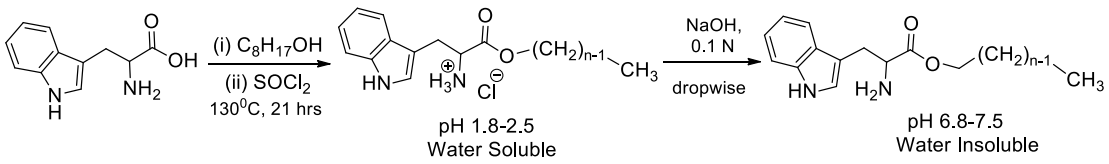

Scheme 2: Synthetic route of L-Tryptophanoctylester (TROE)

The ethyl acetate part was collected over Na_2SO_4 and washed with saturated NaCl solution several times and dried under vacuum for 24 hrs (Scheme 2).[32] The white solid product (TROE) was obtained and characterized using ^{1}H NMR and ^{13}C NMR techniques. Yield of the product was ~92% (8.1 g).

^{1}H-NMR (300 MHz, $CDCl_3$): δ (ppm) 8.2 (s, NH_2), 7.73 (d, 1H, 7.92 Hz), 7.47 (d, 1H, 7.92 Hz), 7.37 (s, 2H), 7.26 (m, 1H), 4.19 (t, 1H, 6.75 Hz), 3.93 (q, 2H, 4.98 Hz), 3.58 (q, 2H, 4.98 Hz), 3.37 (q, 1H, 5.13 Hz), 3.19-3.14 (m, 1H), 1.72 (s, 6H), 1.34 (s, intense, 6H), 0.99 (t, 3H, 6.93 Hz)

^{13}C-NMR (300 MHz, $CDCl_3$): δ (ppm) 171.23, 136.31, 127.46, 123.1, 122.1, 119.46, 118.72, 111.29, 110.92, 65.29, 62.99, 54.91, 31.8, 30.6, 29.4, 29.3, 25.88, 22.66, 14.12.

2.5. Sample preparation

For experiments at low concentration regime (concentration < 5 times critical aggregation concentration (cac)), the aminoacid esters are directly dissolved in water. For experiments at high concentration regimes (concentration > 5 times cac), the samples are dissolved in pure methanol followed by addition of water. The final methanol content in water never exceeded 4%.

3. Results and Discussion

3.1. Molecular modelling of TYOE, TYDE and TROE

Since the geometry of the individual amphiphile molecule determines the packing parameter vis-à-vis morphology of the self-assembled aggregates in aqueous solutions, the structural aspects of TYOE, TYDE and TROE are important and have been studied by density functional theory (DFT) calculations in Gaussian 09 package using the hybrid functional B3LYP and 6-31G as the basis set.[33] According to the above measurements, the most stable conformations of aromatic aminoacid esters are observed as those in which the aromatic moieties are bent/folded towards the hydrocarbon chains at different angles. The optimized conformations of TYOE, TYDE and TROE are shown in Figure 1. The hydrophobic alkyl chain lengths for TYOE, TYDE and TROE as obtained from the DFT calculations are 9.74Å, 14.87 Å and 9.74Å respectively. The respective aromatic planes arise approximately 1.29 Å below the

plane containing the alkyl chain of TYOE and TYDE, and approximately 1.01 Å in case of TROE. The bending angles between the aromatic

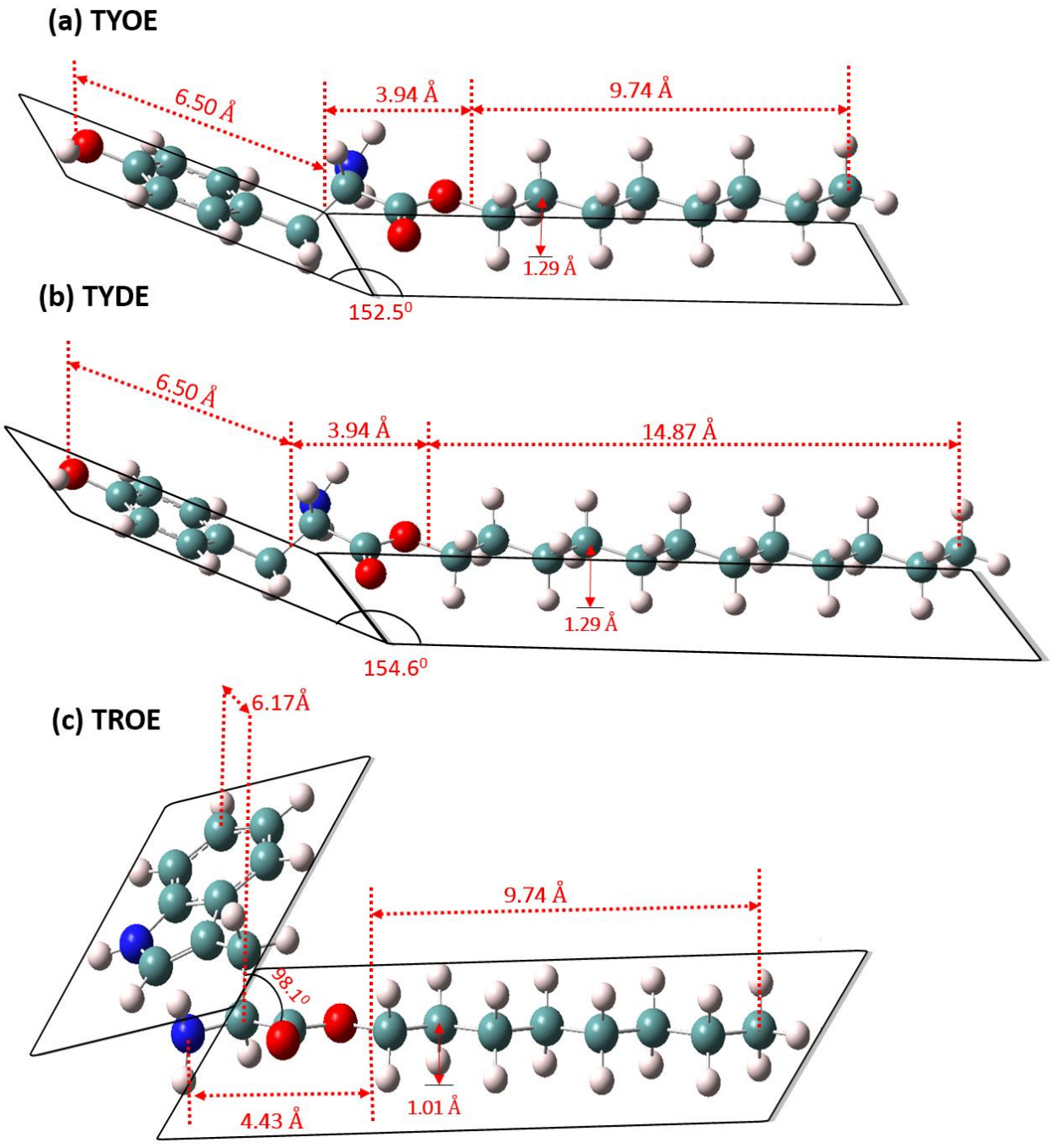

Figure 1. Optimised geometries of (a) TYOE, (b) TYDE, (c) TROE using DFT B3LYP methodology and 6-31G basis set. Color Code: Blue= Nitrogen, Red=Oxygen, Green=Carbon, Grey=Hydrogen

plane and the alkyl chain are 152.5^0, 154.6^0 and 98.1^0 for TYOE, TYDE and TROE respectively. This shows that TYOE and TYDE are comparatively much less aligned (vertically) towards the hydrocarbon skeleton compared to TROE. Single point energy

calculations were done to compute the energetics of the most stable conformation in vacuum. The total thermal internal energy of the most stable conformations i.e., those which display minimum internal energy in vacuum via energy minimization are 280.5 kcal.mol^{-1}, 356.06 kcal.mol^{-1} and 297.55 kcal.mol^{-1} for TYOE, TYDE and TROE respectively. (Theoretical details are provided in Section 1.1 of Appendix B). It is noteworthy that the structural geometry of tryptophan octyl ester was studied previously by molecular mechanics calculation.[28] It has been shown that, in vacuum, the stable conformations were all folded. Extended conformation did occur in water for they were stabilized by electrostatic and Vander Waals interaction between the solvent and TROE molecules. Such interactions are weaker for folded conformations. Nevertheless, there is a difference in potential energy of ~ 5 kcal.mol^{-1} between the extended and folded conformation of TROE in presence of solvent. This again favors the folded conformation.

3.2. Interfacial and bulk properties of TYOE, TYDE and TROE

Measurement of interfacial tension is a reliable and popular tool which provide direct insight into the molecular behaviour of a moiety through careful study of its bulk property. In order to explore the nature of the aminoacid esters, viz., TYOE, TYDE and TROE, in solution, tensiometric study was undertaken. Figure 2 (a-c) shows that the surface tension of water decreases steadily with increasing concentrations of TYOE, TYDE and TROE and reaches a constant value at a critical concentration in each case, like a conventional surfactant. At room temperature, viz., 303 K, sharp break points at 1.81 mM, 1.31 mM and 0.046 mM concentrations of TYOE, TYDE and TROE are observed respectively. The equilibrium surface tension of the solutions at the critical points, (γ_{cac}), are 45.0 mN.m^{-1} for TYOE, 38 mN.m^{-1} for TYDE and 52.5 mN.m^{-1} for TROE. These surface tension values are indeed much lower than that of pure water i.e., 70.8 mN.m^{-1} at 303 K. This result indicates that the aminoacid esters are surface active in nature. The absence of a minimum around the break point confirms the purity of the synthesized ester.[34] Generally, nature of head group and the alkyl chain length of the non-ionic surfactant govern cmc/cac values (cac stands for 'critical aggregation concentration'; the term, in general, is used in this work because of the occasional presence of different types of aggregates together (See Section 3.5)).[35]

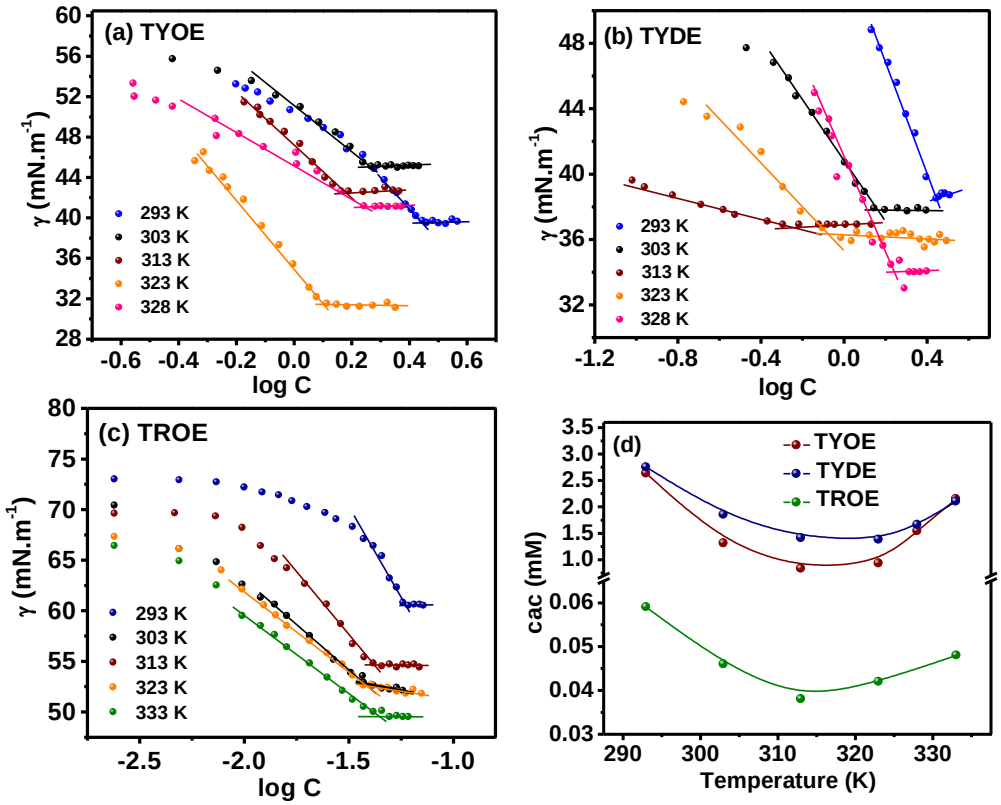

Figure 2. Surface tension profile as function of temperature for (a) TYOE, (b) TYDE, (c) TROE, (d) Variation of cac with temperature for different aminoacid esters.

In the present study, it is observed that the cac values for two tyrosine esters (1.81 mM for octyl and 1.31 mM for dodecyl esters) are not only close to cmc (critical micelle concentration) values normally found for many conventional single tailed surfactants but also follow the well understood trend of synergism as a function of chain length.[36] Tryptophan ester (TROE), however, exhibits surprisingly strong self-assembling tendency in water displaying the cac value of 0.046 mM. The γ_{cac} values for the three aromatic aminoacid esters indicate that none of these amphiphiles packs air-water interface much densely, most probably due to their obliquely bent head group geometry (See also Section 3.4).[37] However, among the three, TYDE molecules are packed most densely while TROE are least densely packed. The pC_{20} values have been determined from the surface tension plots.[38] The pC_{20} is defined as $pC_{20} = - \log C_{20}$, where C_{20} stands for the concentration required to reduce the surface tension of water by 20 $mN.m^{-1}$. The C_{20} is the minimum concentration needed to lead to a saturation of the surface adsorption and thus can be used as the signature for the efficiency of the amphiphile adsorption at the air-water interface. Higher value of pC_{20} imply greater surface active

nature. The pC_{20} values for the present aromatic aminoacid amphiphile systems are found to be 0.05, 0.50 and 1.30 for TYOE, TYDE and TROE respectively. It implies that TROE demonstrates much higher surface activity compared to the tyrosine analogues. The cac of the present systems is a typical weak function of temperature like cmc of the conventional surfactants (Figure 2 (d)).[39] In the present case, it decreases with temperature initially and then increases passing through a shallow minimum. The observed decrease in surface tension is probably caused by orientation of aminoacid esters at the air-water interface. The rapture of hydrogen bonds between the amphiphiles and the water molecules caused by initial rise in temperature, increases the effective hydrophobicity of aminoacid ester molecules, thus favouring its aggregation. The increase in cac at higher temperatures is due to breakdown of the structured "ice-bergs" of water, thus increasing the entropy of aggregation.[40-42] The noted decrease in the equilibrium surface tension values corresponds to higher surface energy with rise in temperature. Other surface parameters underlining the surface behavior of the surface active aminoacid esters in aqueous medium are calculated via Gibbs adsorption equation[43,44] (theoretical background provided under Section 1.2. of Appendix B). and presented in Table 1. The maximum surface excess (Γ_{max}) denotes the number of surface active molecules present at the air-water interface in excess of the bulk. Γ_{max} shows a significant increase of nearly 2.5 times, from 1.96 x 10^{-6} to 4.87 x 10^{-6} $mol.m^{-2}$ in case of TYOE and 2.21 x 10^{-6} to 5.59 x 10^{-6} $mol.m^{-2}$ for TYDE in the temperature range of 323-328 K but in the case of TROE, it decreases from 6.8 x 10^{-6} $mol.m^{-2}$ to 2.6 x 10^{-6} $mol.m^{-2}$ within temperature range of 293-333 K (Table 1). A_{min}, which is the minimum surface area occupied by a molecule at the interface, decreases from 0.85 to 0.46 $nm^2.molecule^{-1}$ for TYOE and 0.75 to 0.46 $nm^2.molecule^{-1}$ for TYDE while increases from 0.24 to 0.66 $nm^2.molecule^{-1}$ for TROE (Table 1). The increase in A_{min} value, in the case on TROE suggests that the molecules are oriented more obliquely at the interface, and explains the decrease in number of excess TROE molecules with temperature. The TYOE and TYDE, on the other hand assume perpendicular orientations and consequently their Γ_{max} is higher.[37] The observation indicates that the head group of the aminoacid ester moieties play a significant role in determining the orientation of the molecules at the interface.

Table 1. Temperature dependence of Critical aggregation concentration (cac), surface parameters viz., surface pressure at cac (Π_{cac}), surface excess, (Γ_{max}), area minimum (A_{min}) of TYOE, TYDE and TROE in aqueous medium

Temperature (K)	cac (mM)	10^3 x Π_{cac} ($mN.m^{-1}$)	10^6 Γ_{max} (mol m^{-2})	A_{min} ($nm^2.molecule^{-1}$)
		TYOE		
293	2.75	33.2	1.96	0.85
303	1.81	26.1	2.55	0.65
313	1.41	26.9	3.45	0.48
323	1.38	36.7	4.87	0.30
328	1.66	25.9	2.55	0.46
		TYDE		
293	2.63	39.6	2.21	0.75
303	1.31	33.4	3.79	0.44
313	0.83	36.9	5.80	0.29
323	0.93	31.8	5.59	0.30
328	1.54	33.1	3.65	0.46
		TROE		
293	0.059	12.6	6.81	0.24
303	0.046	18.3	2.93	0.57
313	0.038	17.8	3.42	0.48
323	0.042	12.8	2.15	0.79
333	0.045	17.7	2.58	0.66

The morphology/phase-transitions of self-assembled aggregates of amphiphilic compounds are dependent on the packing parameter (p),[45]

$$p = v/l.a_0 \ , \qquad (1)$$

where *v* and *l* are the volume and length of the hydrophobic alkyl chain respectively, and a_0 is the area of the hydrophilic head group of the surfactant molecule.

The numerical value of p determines the degree and the extent of morphological transition of the aggregates, formed in surfactant solution. For example, in order to form global micelles, $p \leq 1/3$; for wormlike micelles, $1/3 < p \leq 1/2$; for bilayers, $1/2 < p \leq 1$ and for reverse micelle structures $p > 1$.[46] The effective head group area, $a_{0,}$ of the surfactant molecules, is generally obtained from the variation of the surface tension as a function of concentration[47] and is given by the A_{min} (Table 1). The volume of the

hydrophobic chains, v, can be determined empirically from Tanford's equation as follows-[48]

$$v = 27.4 + 26.9\,n \quad (2)$$

where n is the number of carbon atoms in the chain.

For, n=8 and 12, (for octyl esters of tyrosine and tryptophan and dodecyl ester of tyrosine) v assumes the values of 242.6 $Å^3$ and 350.2 $Å^3$ respectively. Using these values, and the value of A_{min} from Table 1, assuming perpendicular orientation only, p is found to be 0.38 for TYOE, 0.53 for TYDE and 0.43 for TROE. The values indicate that in the case of TYOE, p is slightly above the limit of 0.33 (for micelles), and therefore, is expected to aggregate as nearly spherical micelle as well as ellipsoidal clusters, while both TYDE and TROE would have strong inclination to pack as bilayers or vesicles.[49]

3.2.1. Thermodynamics

The energetics of aggregation and interfacial adsorption have been studied as function of temperature (Table 2) using Gibbs adsorption isotherm[34] and Mass action model [50] of surfactant aggregation respectively. Mathematical details and equations are provided under Section 1.2.1 in Appendix B. The standard free energy of aggregate formation per mole of monomer unit [51] for TYOE, TYDE and TROE in aqueous medium is evaluated based on Mass action model and summarized in Table 2. The high negative ΔG^0_{agg} for TROE aggregation, compared to that for tyrosine analogues, shows that the aggregation process is much favored in the former. The self-assembly of amphiphilic molecules in polar solvents like water generally involves interesting thermodynamic maneuver.

Table 2. Thermodynamic parameters viz., Standard Gibbs free energy change of aggregation (ΔG_{agg}^0), standard enthalpy change of aggregation (ΔH_{agg}^0),standard entropy change of aggregation (ΔS_{agg}^0) and standard free energy change of adsorption (ΔG_{ads}^0) of TYOE, TYDE and TROE in aqueous medium.

Temperature (K)	ΔG_{agg}^0 (kJ.mol^{-1})	ΔH_{agg}^0 (kJ.mol^{-1})	ΔS_{agg}^0 (J.mol^{-1} K^{-1})	ΔG_{ads}^0 (kJ.mol^{-1})
		TYOE		
293	-10.33	+56.56	+228.31	-27.24
303	-12.29	+38.41	+167.31	-22.51
313	-14.48	+16.73	+99.17	-22.27
323	-13.27	-8.56	+14.59	-20.81
328	-13.22	-22.77	-29.11	-23.40
		TYDE		
293	-11.42	+36.19	+162.50	-29.34
303	-12.88	+17.74	+101.08	-21.69
313	-13.55	+0.78	+45.78	-19.91
323	-13.48	-15.65	-6.71	-19.17
328	-14.17	-30.63	-50.17	-23.23
		TROE		
293	-33.51	-9.32	+82.55	-35.36
303	-35.89	-9.05	+88.58	-42.21
313	-36.94	-7.71	+93.38	-42.18
323	-37.85	-6.12	+98.23	-43.94
333	-38.89	-4.31	+103.84	-45.97

On the one hand, the endothermic melting of the ordered solvent cluster due to hydrophobic effect of the amphiphile dominates over the exothermic association of hydrophilic parts leading to positive entropy change. The hydrophilic part, on the other hand, preferentially hydrates in solvent water via hydrogen bond formation with water molecules. Thus a greater enthalpic compensation is brought about compared to that if the hydrophilic parts are interacted among each other leading to electrostatic repulsion between adjacent hydrophobic blocks. The balance between all such forces drives the formation of aggregates of different size, shape and order. Thus, during aggregation, compared to tyrosine analogues, the endothermic melting of ordered water molecules around nonpolar tail of TROE is much greater than the subsequent exothermic assembly of the molecules (Table 2). While hydrophobic and electrostatic interactions

dominate ΔH^0_{agg}, ΔS^0_{agg} is contributed by the transfer of the hydrocarbon chains of the monomers into the aggregate core.[52] Thus temperature favors the decrease of the exothermic repulsion between the tryptophan head groups in TROE. Further, the association of monomers, readjustment of the hydration sphere of the head groups within the aggregates and reorganization of the hydrocarbon chains at the aggregate core increases the overall degrees of freedom of the system causing a net rise in entropy.[53] The linear enthalpy-entropy compensation relationship was observed with compensation temperature, T_c, as 308 K, 313 K and 246 K for TYOE, TYDE and TROE respectively (Figure S1 of Appendix B). Further, the negative values of ΔG^0_{ads} indicate that the phenomenon of interfacial adsorption is also spontaneous in nature. In the case of TYOE and TYDE, ΔG^0_{ads} shows a non-regular trend with temperature while in the case of TROE, the value increases as function of temperature. This shows that temperature favors the process of adsorption in TROE. Furthermore, the more negative values of ΔG^0_{ads} compared to ΔG^0_{agg} for TYOE, TYDE and TROE at all temperatures indicate that the adsorption process in all the aminoacid esters is more spontaneous in comparison to their corresponding aggregation.[44]

3.2.2. Steady state fluorescence emission

Steady state fluorescence emission study was performed in order to verify cac values of the aminoacid aggregates and to ascertain the microenvironment of the molecular aggregates in solution. Figure 3 (a) depicts the variation of fluorescence emission intensity of 2 µM aqueous pyrene solution upon increasing concentration of TYOE (representative plot). Plots for TYDE and TROE are provided in SI (Figure S2 of Appendix B). The lowering of emission intensity signify considerable binding of pyrene to the TYOE molecules. The relative intensities of the vibronic bands, I_1/I_3, of pyrene emission are plotted as function of the concentrations of aminoacid esters (Figure 3 (b)).

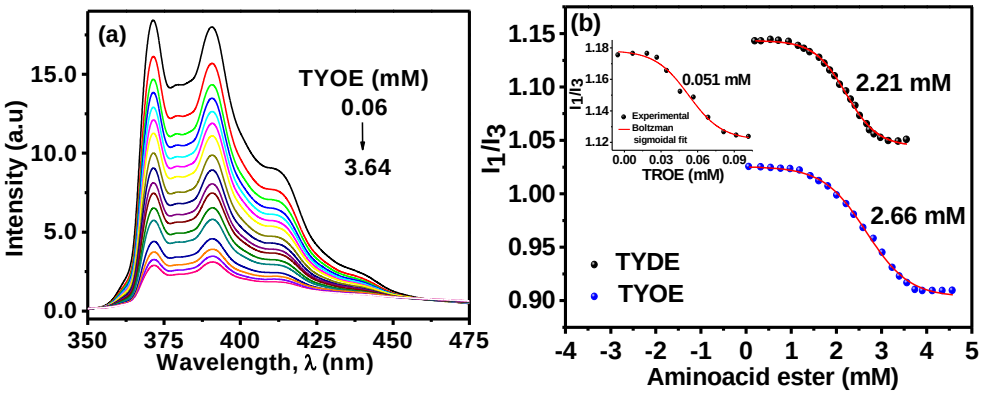

Figure 3. (a) Variation of emission intensity of 2µM aqueous Pyrene as a function of TYOE concentration at 303 K (representative plot), (b) Relative intensities of vibronic band (I_1/I_3) of pyrene fluorescence in aqueous solution of TYOE, TYDE and TROE at 303 K. Solid circles - experimental curve, Dashed line - Boltzmann sigmoidal fit.

A sigmoidal variation is observed in all the three cases (Figure 3(b)). The values were fitted according to Boltzman distribution to obtain the inflexion point, which has been considered as the cac.[54] The cac's obtained by this method are 2.66 mM for TYOE, 2.21 mM for TYDE and 0.051 mM for TROE respectively. These values differ to a considerable extent from those obtained from the surface tension measurement (Table 1). However, such difference of results of the two methods are not uncommon.[6] The I_1/I_3 value, which is shown to be the measure of the polarity of the fluorophore location, ranges from 0.91 to 1.02 in TYOE, 1.04 to 1.14 in TYDE and 1.12 to 1.18 in TROE (Figure 3(b)). The values are consistent with those observed for pyrene in non-polar solvent toluene (1.11) and in non-polar micellar core of traditional anionic surfactant Sodium dodecyl sulfate (1.14).[54] The vibronic bands of the fluorescence emission spectrum of pyrene are highly sensitive to the local polarity; the I_1/I_3 values in micelle-solubilized pyrene increases with solvent polarity.[55] Therefore, it is evident that the pyrene molecules partition into a preferably non-polar location at core of the aggregates. This also corroborates the fact that the lowering of the emission intensity upon increased amphiphile concentration as observed in Figure 3(a), is the signature of partitioning more and more fluorophore into the aggregate core. Further, I_1/I_3 varies in the order TYOE>TYDE>TROE, implying that the aggregate core is more polar in TROE followed by TYDE and least polar in TYOE.

3.2.3. Aggregation Number

The steady-state fluorescence quenching technique was used to determine the aggregation number (N_{agg}) of the aggregates of aminoacid esters. The equilibrium of the aminoacid esters between the aqueous and the self-assembled pseudo-phases follows the Poisson distribution. The following equation is applied to analyze the fluorescence quenching data[56]

$$\ln I = \ln I_0 - \frac{C_Q}{C_a} \quad (3)$$

$$\text{Or, } \ln I = \frac{\ln I_0 - N_{agg.} C_Q}{C_T - cac} \quad (4)$$

where C_Q, C_a, and C_T are the concentrations of quencher, aggregate, and total aminoacid esters, respectively, while I and I_0 are the fluorescence intensities in the presence and absence of the quencher. Figure 4 shows the emission spectra of pyrene in aqueous solutions of the aminoacid esters in the presence of varying quencher concentrations (Cetylpyridinium chloride, CPC). The emission intensity of pyrene decreases with the increase of quencher concentration in all the three aminoacid esters. From the slope of the plots of ln (I/I_0) vs. quencher concentration (Insets of Figure 4(a), (b) and (c)) and the cac values, the N_{agg} is determined by using Equation 4. In order to avoid the possibility of microstructure transition, concentration of amphiphile is kept 4.5 times of cac, whereas higher concentration is usually desirable. However, the results of the quenching experiment suggests that, both pyrene and the quencher, CPC, are partitioned well within the aggregate core under above concentration condition. The shape of the emission spectra of pyrene is modified in presence of CPC; the vibronic structure becomes ill-defined and the spectra is red-shifted due to the interaction of pyrene molecules with the pyridinium head groups of CPC within the aggregates. The aggregation numbers obtained by this method are 35 and 18 respectively for TYOE and TYDE, while that for TROE, N_{agg} could not be determined due to nonlinear nature of the ln (I/I_0) vs. quencher concentration plot (Inset of Figure 4(c)). It seems apparent that the experimental plots (insets of Figure 4 (a) and Figure 4 (b)) for TYOE and TYDE are consistent and yield the values of $N_{agg.}$ Nevertheless, the aggregation numbers are unusually small, especially for TYDE aggregates. Moreover, the deviation of plots of ln (I/I_0) vs. quencher concentration (for TROE), from linearity is undoubtedly indicative of morphology transition of the aggregates at the experimental concentration. It is

therefore tempting to examine the molecular interaction (by 2D NMR) and detail morphology (by HRTEM) at similar and higher concentration regimes of the aminoacid analogues.

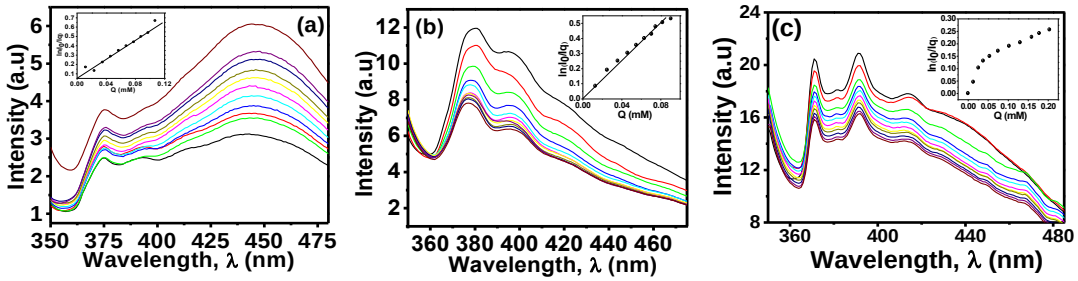

Figure 4. Variation of fluorescence emission spectra of 2µM Pyrene in aqueous solutions of the amino (a) 8.09 mM TYOE, (b) 4.24 mM TYDE, (c) 0.21 mM TROE at 303 K. Insets display linear plots of ln (I/I_0) for 2µM Pyrene in aqueous solutions of the respective aminoacid esters as function of Cetylpyridinium chloride (Q) concentrations.

3.4. Molecular interactions: 2D NMR (Concentration > 5 fold cac)

Nuclear magnetic resonance (NMR) spectroscopy is a powerful and reliable tool for the investigation of molecular aggregates.[57] The NMR techniques have been successfully utilized in determining parameters like size, shape, degree of association, structure etc. of various self-assemblies.[58-61] Rotating frame Nuclear Overhauser effect spectroscopy (ROESY) is one of the 2D NMR techniques which correlates signals arising via dipolar interaction from protons that are close in space (<5Å). The intensity of cross peaks of ROESY spectra reflects the extent of magnetization transfer between the nuclei and is proportional to the internuclei distance.[62] Herein, 2D ROESY spectroscopic analysis is utilized to study the microstructure of the aminoacid esters, viz., TYOE and TROE in solution (D_2O). The chemical representation and proton numbering of TYOE and TROE are shown in Scheme 3.

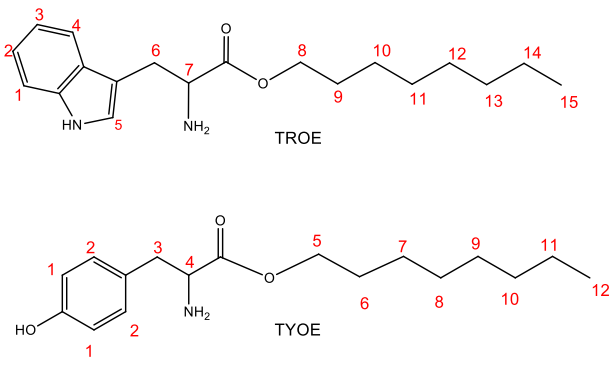

Scheme 3. Chemical representation and proton numbering of TROE and TYOE

The presence of key cross peaks in the ROESY spectra of TYOE and TROE (Figure 5) suggests that strong interaction occurs between various protons of the respective molecules. In Figure 5(a), the intense cross peaks 3/4-15 and 1/2-15 correlate the aromatic protons of the indole ring of tryptophan moiety with the terminal alkyl protons.

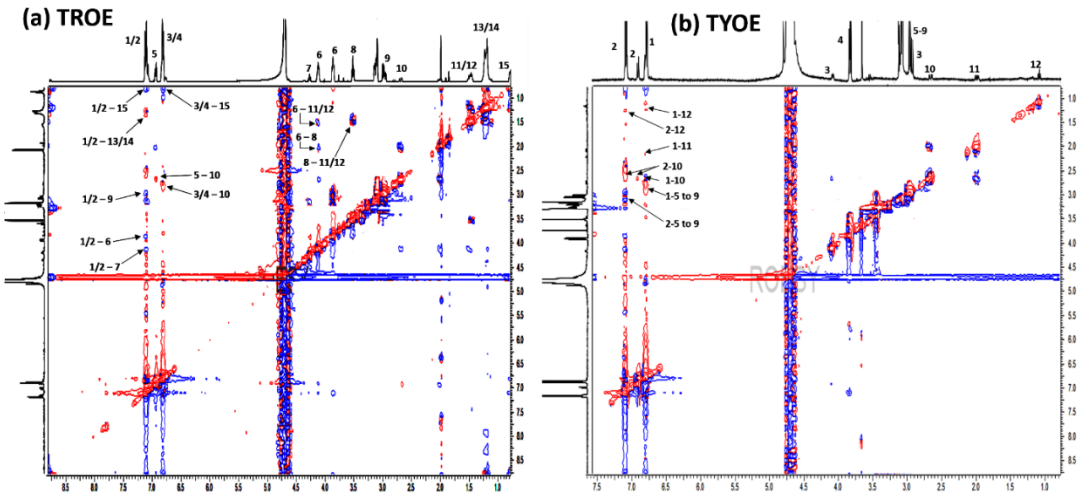

Figure 5. 2D ^{1}H-^{1}H ROESY spectra of (a) TROE (0.5 mM), (b) TYOE (7.2 mM) in D_2O at 303K.

Cross peaks viz., 1/2 -13/14, 3/4-10 and 1/2-9 are observed between the aromatic protons and the intermediate aliphatic protons of the octyl chain of TROE. These correlations suggest that the aromatic face of the TROE molecule containing the benzene ring of the indole moiety lie in close proximity of the aliphatic protons of the alkyl chain of TROE, including the terminal methyl protons. The optimized geometries of aminoacid esters (Section 3.1) in vacuum especially that of TROE, also showed that aromatic ring remains folded. Previously, theoretical studies using molecular mechanics calculations,[28] have shown that an extended conformation of TROE molecule is energetically unfavorable and that TROE molecule exist as folded conformer in vacuum as well as in water box, with the amino and carboxylate groups located at one end creating a polar extremity. Similar conformation of TROE is observed herein from the ROESY spectrum. The interaction of aromatic protons with terminal methyl group further suggests that the aliphatic chain tend to bend towards the aromatic ring exhibiting a folded structure. Strong hydrophobic interactions between the aromatic ring and the aliphatic chain might be the driving force behind the “bending inwards” of the terminal alkyl protons and the observed cross-peaks in ROESY spectrum. This conformation of TROE may be stabilized by the favorable vander Waal

interaction and possible hydrogen bonding between the solvent water molecules and the polar amino and carboxyl groups of TROE, which lie at the micellar interface. Furthermore, the two H6 protons exists in two magnetically non-equivalent environment. One is closer to the polar amino group and appear downfield at δ 4.2 ppm while other is oriented away from the amino group and appear relatively upfield at δ 3.9 ppm (Figure S3 (a) of Appendix B). In ROESY spectrum, a correlation between the more downfield H6 proton is observed with H8 and H11/H12 proton of the alkyl chain. Moreover, several other weak cross peaks viz., 1/2-6, 1/2-7 and 5-10 are also observed correlating the aromatic protons with the protons at the polar end of the head group. These interactions, suggests that molecular interactions may also occur between two adjacent TROE molecules.

In the case of TYOE, two fascinating aspects were observed. Firstly, in spite of consisting of two types of magnetically non-equivalent aromatic protons viz., H1 and H2 (Figure 5(b)), the ^{1}H NMR spectra displayed low intensity resonance signals for a third type aromatic proton at δ 7.00 ppm (Figure S3 (b)). This indicates that some of the H2 protons may be hydrogen-bonded to the amino group in its vicinity. The 2D ROESY spectrum reveals that this hydrogen-bonded proton interacts with H10 of the aliphatic chain giving rise to cross peak at 6.99-2.75. A very weak correlation peak is observed between the aromatic H1 proton and the terminal methyl protons viz., H12. This shows that the aliphatic chain terminal is located away from the proximity of the aromatic ring contrary to that observed in TROE. Secondly, unlike commonly observed for aliphatic proton resonances and as observed in the spectra of TYOE in non-polar solvent $CDCl_3$ where it appears at δ 1.33 ppm (Figure S3 (a) of Appendix B), the chain protons H5-H9 appears highly downfield in D_2O and merges into a single peak observed at 3.16 ppm (Figure S3 (b) of Appendix B). No intense peak at the non-polar end suggesting otherwise is evident. The observation indicates that the chain protons of TYOE experiences unusually high polar environment in aqueous medium compared to TROE. Intense cross-peaks correlating these protons viz., H5-H9 with the aromatic non-bonded H2 proton is observed. It seems likely that in TYOE, the aromatic moiety bends inwards the carbonyl group along with the ester–oxygen facing the interface.[63] Due to incorporation of rigidity in structure owing to the hydrogen bonding, the aromatic group remain less closely packed compared to TROE. The highly polar environment experienced by H5-H9 in TYOE may be explained by the close proximity

of the $–NH_2$ group in the vicinity, as well as the presence of larger number of the polar solvent molecules compared to TROE.

On basis of the 2D NMR observation, a probable structure of TROE and TYOE as present within the aggregates and the intra-molecular interaction between different protons is shown in Scheme 4.

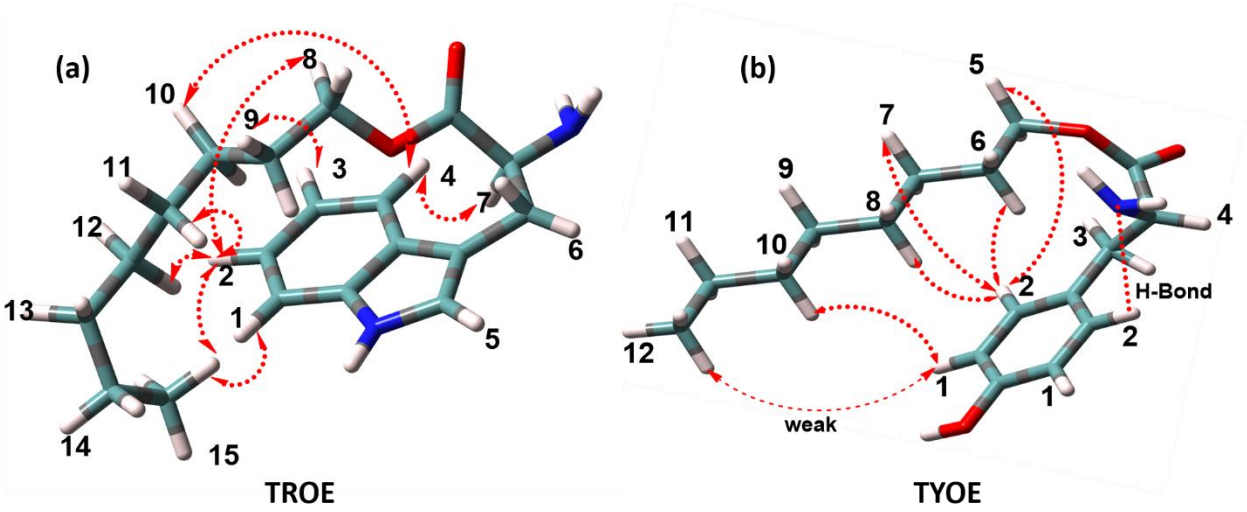

Scheme 4. Key ^1H-^1H intra-molecular ROESY (⟷) correlations in (a) TROE and (b) TYOE. Color code: Blue= Nitrogen, Red=Oxygen, Green=Carbon, Grey=Hydrogen

3.5. Morphology of aggregates: HRTEM and DLS (Concentration >5 fold cac)

The aggregate morphology of the aminoacid esters were visualized using High Resolution Transmission Electron Microscopy (HRTEM)[6] (Figure 6). To ensure complete aggregation and microstructure transformation, aqueous solutions of the aminoacid esters were prepared with concentrations 5-10 times of their respective cac. The TEM micrographs show presence of aggregates of different sizes having diverse microstructural features. In TYOE, spherical micelles of size 5-10 nm (representative indication by red square) and small spherical vesicles of size 20-30 nm (representative indication by red arrow) are observed to pack together in form of ellipsoid domains (Figure 6 (a)).

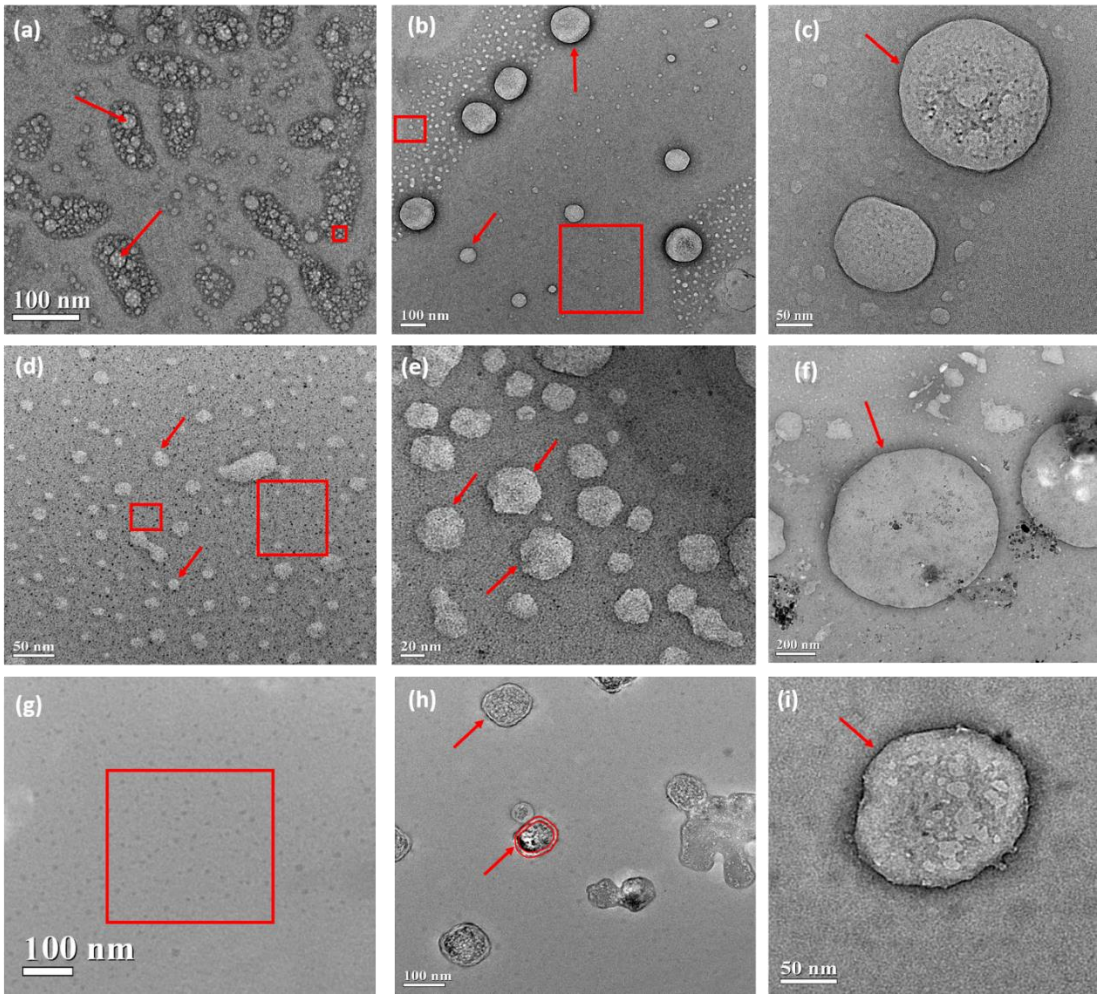

Figure 6. HRTEM micrographs of (a-c) 7.2 mM TYOE in aqueous medium in different fields of view: (a) shows the clusters of vesicular aggregates, (b) Boxes highlight dispersed micellar aggregates, size < 10nm. Arrows indicate presence of large vesicles of diameter >50 nm. (c) Presence of giant spherical vesicles of diameter ~200 nm; (d-f) 9.0 mM TYDE in different fields of view: (d) presence of aggregates of micellar dimension (arrows and boxes), (e) Mesosize aggregates with regular hollow internal structures (Trigonal dodecahedron/icosahedron?), (h) Giant vesicle of diameter ~200nm (g-i) 0.5 mM TROE in different fields of view: (g) uniformly distributed micellar aggregates, (h) vesicles with distinct bilayer membrane of thickness ~5-7 nm of predominantly square geometry, Hollow concentric circles indicate bilayer thickness. (i) Large spherical vesicle of diameter ~ 150 nm.

Furthermore, the vesicles form stacked-up structures, as is evident from their overlapped contour (indicated by red arrow).[64,65] Absence of well-defined membrane around the periphery of the large ellipsoidal assembly suggests that the formation of this cluster is driven by solvophobic repulsive interactions between the micelles or vesicles and the solvent molecules. It may also be seen that large spherical vesicles, of average diameter of ~100 nm are present alongside the smaller micellar aggregates which are dispersed throughout the field of view (Figure 6 (b)). Larger vesicles of diameter > 200 nm are also present (Figure 6 (c)). Similar co-existence of small micelles (size <8 nm) and vesicles (diameter 20-25 nm) is evident in TYDE (Figure 6 (d)) as well. Closer inspection of HRTEM picture of TYDE aggregates reveals the presence of mesosize aggregates with regular hollow internal structures, which look like trigonal dodecahedron/icosahedron geometry (Figure 6 (e)). The aggregates in TYDE are spheroidal and have diameter ~10-20 nm. These are comparatively more homogeneously distributed (Figure 6 (d)) than TYOE. Besides, there are large number of smaller aggregates of micellar dimension (black dots), evenly distributed within the field of view (Figure 6). However, giant spherical vesicles (diameter ~200 nm) similar to that in TYOE are also observed in TYDE (Figure 6 (f)). In TROE, micellar aggregates of size <10 nm are found dispersed in the medium (Figure 6 (g) indicated by red square), while larger vesicles of average dimension ~60-80 nm, having cubic geometry (indicated by red arrow) are found to co-exist (Figure 6 (h)). Giant vesicles similar to those in TYOE and TYDE are also observed in another field of view (Figure 6 (i)). The membrane bilayer thickness observed in larger vesicles of TYOE, which are relatively less abundant than the smaller ones, is about ~4-6 nm. The TROE consisted of large vesicles with well-defined bilayer boundaries. The bilayer membrane thickness of TROE was ~8-10 nm. The vesicles of TROE are sparsely distributed compared to TYOE and TYDE, and this may be due to much lower concentration of TROE (0.5 mM) compared to TYOE (7.2 mM) and TYDE (9 mM) of the experimental samples.

The presence of the large vesicular aggregates in TYOE, TYDE and TROE was also examined using the dynamic light scattering measurements (DLS), at 303 K (Figure 7). For better understanding, the sample concentrations were kept identical to that used during HRTEM measurement. It is evident that giant aggregates of size 200 nm – 600 nm are present in all the three aminoacid esters. The average hydrodynamic diameter (d_h), of TYOE, TYDE and TROE are obtained as 451 nm, 353 nm and 540 nm

respectively. The results confirm the aggregation of the aminoacid esters into giant vesicles.

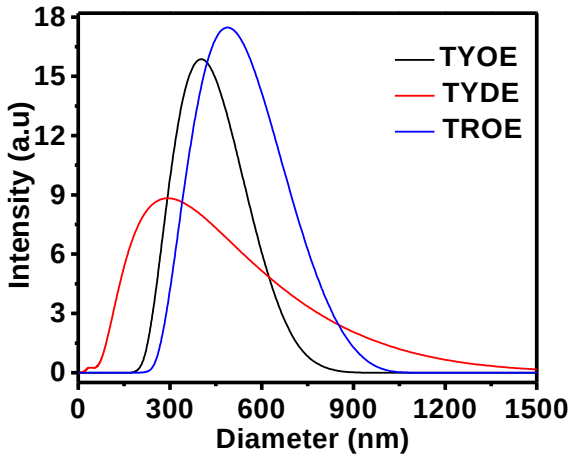

Figure 7. Size distribution of aggregates in aqueous solutions of 7.2 mM TYOE, 9.0 mM TYDE and 0.5 mM TROE as obtained from DLS measurement at 303 K.

Unlike conventional single tailed surfactant systems, TYOE, TYDE and TROE aggregates display rich morphologies as observed from HRTEM study in the absence of any promoter/additive. The key difference of aromatic aminoacid esters from the conventional surfactants is that unlike the later, aminoacid esters contain blocks of hydrophobic and hydrophilic moieties in their molecular structures. This molecular picture is similar to that one witnesses in block copolymer amphiphiles, the self-assembled aggregates of which have attracted wide interests due to creation of a plethora of morphologies.[17,65,66] For these systems which contain multiple number of hydrophobic and hydrophilic blocks, the morphologies are determined by the curvature created in the assembly via relative volume of such water insoluble and water soluble domains. The balance between the hydrophobic and hydrophilic interactions give rise to an optimum surface area (a_0) of hydrophobic block at the interface between hydrophobic and hydrophilic domains. This area, together with the length and volume of hydrophobic block contributes to the packing parameter. In the present amphiphilic systems, viz., TYOE, TYDE and TROE, containing hydrophobic and hydrophilic blocks in the molecule, the geometries and degree of order of the aggregate nanostructures depends on the amphiphile concentration as well as the volume ratio of the water insoluble and water soluble blocks – 'the insoluble soluble ratio (ISR)'.[66,67] As a result, at low concentration, due to the soluble domain compatibility with the solvent, the system may be soluble. On the other hand, at the cac or higher

concentrations, the molecules containing multiple number of blocks self-assemble to form either dispersed isotropic globular phase or larger aggregates with higher order morphology. From the length of hydrophobic and hydrophilic domains for TYOE, TYDE and TROE, as determined by DFT calculations (Figure 1), the corresponding ISR values for these amphiphiles are found to be 4.12, 5.42 and 3.93 respectively (assuming identical cross-sectional area). It may, therefore, be presumed that the surface activity of the above systems would be in the order TYDE > TYOE > TROE, unless major structural discrimination is encountered by them in presence of polar solvent.

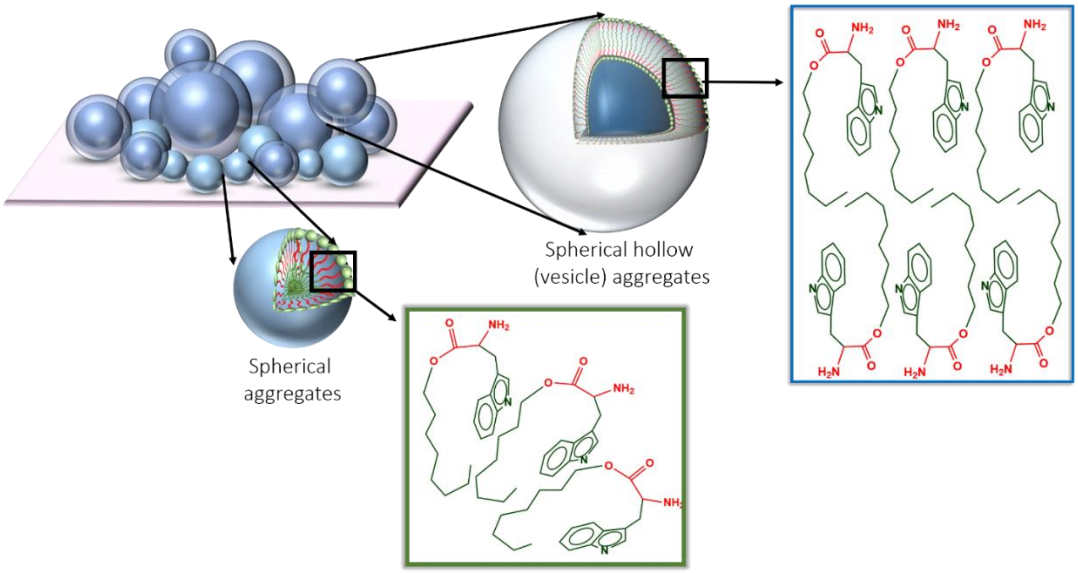

Scheme 5. Schematic representation of possible morphology and orientation of L-Tryptophanoctyl ester molecules in bilayer and micelles.

However, due to segregated structure in presence of solvent, present system deviate from above trend. Therefore, instead of kinetically trapped non equilibrium structures of small vesicles formed by conventional double tailed surfactants with inverted cone/truncated cone like molecular form, thermodynamically stable vesicles and bilayers are formed in present amphiphile systems due to their intrinsic polydispersity. Such polydispersity leads to selective segregation of hydrophobic blocks to the inside of vesicles, whereas hydrophilic blocks segregates to the outside. The preferred curvature of the bilayer is stabilized in this way. The effect is enhanced in smaller vesicles since the tendency to segregate would be greater as interfacial curvature is increased. The various morphologies that are observed in the present systems are primarily a result of inherent molecular curvature of these and how this influences the packing of the amphiphiles in the assemblies. A schematic representation of possible

morphology and orientation of the molecules in bilayer and micelles is shown in Scheme 5. The vesicles which are formed in the present aminoacid ester based amphiphile systems are found to be stable (examined up to 10 days and found stable in terms of size). The conformation of individual aminoacid ester molecule as observed by DFT computation is modified in aqueous aggregates. As is revealed from 2D NMR study, these molecules are further folded in the aggregates due to the interplay between hydrophobic and hydrophilic forces including H-bonding between the polar groups present in the hydrophilic blocks with the water molecules at the interface. Therefore, the driving force of the self-assembly formation is the hydrophobic and hydrophilic interactions along with the non-covalent interactions including H-bonding. The thermodynamic maneuver (enthalpy and entropy) plays a vital role just like the aggregation process as involved in block copolymers and common surfactants in polar solvents. Hydrogen bond formation in aqueous amphiphilic systems have attracted much attention recently, both experimentally and theoretically, because it has been proved of crucial importance on the structural and dynamic properties of self-assembled nanostructural motifs.[67] The array of intramolecular and intermolecular interactions among the blocks within TYOE, TYDE and TROE assemblies in water generates the sophisticated structures. These interactions for the formation and stability of rich morphologies also undoubtedly includes H-bonding network that is formed among interfacially located hydrophilic blocks as well. The difference between the molecular packing predicted from Israelachvili's approach[46] (Section 3.1) and that observed in solvent is, therefore, due to the molecular folding induced by the solvent. In presence of solvent, the aminoacid esters, with the folded aromatic ring behave as the pseudo-double tailed surfactants with truncated cone geometries and the hydrophilic blocks oriented towards the interface act as the "head groups". Such orientation is favored due to strong hydrogen bonding of the polar head groups with the solvent water molecules.[67] Therefore, due to molecular folding in presence of water vis-à-vis segregation of hydrophobic and hydrophilic blocks, the conventional approach of the calculation of packing parameter and the prediction of aggregation morphology in terms of individual molecular geometry is not valid, and hence, does not follow in the present study.[68]

4. Conclusion

Molecular geometries of the models for membrane proteins, viz., TYOE, TYDE and TROE, as determined via energy minimization by DFT calculations, exhibit partial

bending of the aromatic ring (phenol or indole respectively) towards hydrocarbon chain of the molecules. Occurrence of a hydrophilic block (consisting of ethereal oxygen, carbonyl and the amine groups) between two strongly hydrophobic blocks (consisting of phenol/indole ring and the hydrocarbon chain respectively) in the molecular architectures and the obliquely bend molecular geometry leads to form a distinctive amphiphilic system that unveil strong surface active properties in aqueous solutions. The 2D NMR in D_2O reveals that the unique molecular geometry of these tyrosine and tryptophan analogues facilitate strong segregation domain of the two hydrophobic blocks to form within the same molecule and this leads to further folding of the molecules via non-covalent interactions including hydrogen bonding. The display of rich morphology of the exclusive aggregates, as has been witnessed in the present systems, is not only rare for single chain amphiphiles, the biocompatibility of the aromatic aminoacid esters make them highly potential contender for drug delivery vehicle and drug vectors as well. The demonstration of chemically segregated domains with exceptional chemistries and topographies, leading to the formation of bilayer and membrane motifs commands fundamental features of cell membranes and may have important relevance in biotechnology. Further, it points out to the fact that membrane proteins are not just integral dopants in the membrane system but very much set its role as the building blocks of the cell membrane and may act as the stabilizer of the membrane structure as well.

References are provided in BIBLIOGRAPHY under "References for Chapter V" (Page 178-183)

Findings of this chapter has been published in *Langmuir*, **2017**, 33, 6581-6594.